Available online at www.sciencedirect.com

ScienceDirect

www.elsevier.com/locate/jes

JES JOURNAL OF ENVIRONMENTAL SCIENCES

www.jesc.ac.cn

Wall losses of oxygenated volatile organic compounds from oxidation of toluene: Effects of chamber volume and relative humidity☆

Shanshan Yu[1,2], *Long Jia*[1,2,*], *Yongfu Xu*[1,2], *Hailiang Zhang*[1,2], *Qun Zhang*[1,2], *Yuepeng Pan*[1,2]

[1] *State Key Laboratory of Atmospheric Boundary Layer Physics and Atmospheric Chemistry, Institute of Atmospheric Physics, Chinese Academy of Sciences, Beijing 100029, China*

[2] *Department of Atmospheric Chemistry and Environmental Sciences, College of Earth and Planetary Sciences, University of Chinese Academy of Sciences, Beijing 100049, China*

ARTICLE INFO

Article history:
Received 10 May 2021
Revised 14 September 2021
Accepted 24 September 2021
Available online 22 February 2022

Keywords:
Vapor wall loss
Surface-to-volume ratio
Relative humidity
Toluene
Smog chamber
Oxygenated volatile organic compounds

ABSTRACT

Vapor wall losses can affect the yields of secondary organic aerosol. The effects of surface-to-volume (S/V) ratio and relative humidity (RH) on the vapor-wall interactions were investigated in this study. The oxygenated volatile organic compounds (OVOCs) were generated from toluene-H_2O_2 irradiations. The average gas to wall loss rate constant (k_{gw}) of OVOCs in a 400 L reactor (S/V = 7.5 m^{-1}) is 2.47 (2.41 under humid conditions) times higher than that in a 5000 L reactor (S/V = 3.6 m^{-1}) under dry conditions. In contrast, the average desorption rate constant (k_{wg}) of OVOCs in 400 L reactor is only 1.37 (1.20 under humid conditions) times higher than that in 5000 L reactor under dry conditions. It shows that increasing the S/V ratio can promote the wall losses of OVOCs. By contrast, the RH effect on k_{gw} is not prominent. The average k_{gw} value under humid conditions is almost the same as under dry conditions in the 400 L (5000 L) reactor. However, increasing RH can decrease the desorption rates. The average k_{wg} value under dry conditions is 1.45 (1.27) times higher than that under humid conditions in the 400 L (5000 L) reactor. The high RH can increase the partitioning equilibrium timescales and enhance the wall losses of OVOCs.

Introduction

Secondary organic aerosol (SOA) accounts for a significant portion of fine particles, which adversely affects visibility, climate and health (Steinfeld, 1998; Liao et al., 2007; Pan et al., 2017; Suda et al., 2014). SOA is mainly formed by gas-particle partitioning of semi-volatile organic compounds (SVOCs) produced by atmospheric oxidation of volatile organic compounds (VOCs) (Grieshop et al., 2009; Huffman et al., 2009) and particle-phase reactions (Chen et al., 2021; Huang et al., 2016; Kroll et al., 2007; Liu et al., 2019).

Smog chambers are widely used to investigate atmospheric chemistry (Chen et al., 2019; Shi et al., 2019; Song et al., 2019; Wang et al., 2014, 2015). The vapor wall loss has attracted lots of attention due to its foundation influence in the interaction with particles and gaseous oxidation products (Bertrand et al., 2018; Kokkola et al., 2014; Krechmer et al., 2016, 2017; La et al., 2016; Matsunaga and Ziemann, 2010; McVay et al., 2014; Nah et al., 2016; Yeh and Ziemann, 2014, 2015; Zhang et al., 2014, 2015). Some researchers partly at-

☆ This article is dedicated to Professor Dianxun Wang.

* Corresponding author.
E-mail: jialong@mail.iap.ac.cn (L. Jia).

https://doi.org/10.1016/j.jes.2021.09.026
1001-0742/

tributed the low yields of SOA to the wall losses of oxygenated volatile organic compounds (OVOCs) (Kroll et al., 2007; Pathak et al., 2008). Zhang et al. (2014) found that vapor wall loss could indeed cause an underestimation of chamber-derived toluene SOA mass yields by a factor of 4. Grosjean and co-workers (Grosjean, 1985; McMurry and Grosjean, 1985) determined the wall loss constants of several VOCs in a 3.9 m^3 reactor and found that the lifetimes of these molecules were generally larger than 15 hr. Ziemann and co-workers (Matsunaga and Ziemann, 2010; Yeh and Ziemann, 2014, 2015) determined the wall losses of intermediate volatile organic compounds (1-alkenes, ketones, alcohols, monoacids and diols and alkyl nitrates). They found that the vapor wall loss was a reversible process with an equilibrium time of tens of minutes. Finewax et al. (2020) measured the vapor-wall losses of 2-ketones (n_C = 7 - 13), and the equilibrium timescales were determined to be about 13 min. These studies directly determined the wall losses of OVOCs using the surrogate species. Actually, hundreds of OVOCs with various molecular weights and functional groups could be produced during VOC oxidation. It may be challenging to find suitable surrogate species to represent complicated species from oxidation of a specific VOC in the chamber study. Thus, it is necessary to measure the wall losses of OVOCs directly from the in situ oxidation of VOC. Recently, the in-situ reaction has been used to study the wall losses of compounds. Zhang et al. (2015) measured the wall deposition rates of OVOCs from the oxidation of α-pinene, n-dodecane, toluene and isoprene, with initial irradiation times varying from 1 to 7 hr. Krechmer et al. (2016) determined the wall losses of the OVOCs generated by in-situ oxidation of 1-alcohols (n_C = 6 - 12).

Relative humidity (RH) is a key factor controlling water distribution between the gas and particle phases. OVOCs generally contain polar functional groups and are water-soluble, and thus RH conditions may affect the vapor-wall interactions of OVOCs. There are only limited reports on RH-dependent vapor wall loss rate (Bates et al., 2014; Huang et al., 2018; Loza et al., 2010; Nguyen et al., 2016, 2014). Loza et al. (2010) found that the wall loss rate constant of glyoxal at 61% RH was two orders of magnitude higher than that at RH < 10%; While the wall loss rate constant of 2, 3-epoxy-1,4-butanediol at 45% RH was about 2 times higher than that at 10% RH. Huang et al. (2018) compared the humidity effect on the wall losses of two isoprene oxidation products ($C_5H_8O_2$ and $C_5H_9O_4N$). They found that $C_5H_9O_4N$ exhibited a faster decay rate at 50% RH than $C_5H_8O_2$ due to containing a -ONO_2 group. Toluene is an important SOA precursor. To the best of our knowledge, the effects of RH on OVOCs wall losses from toluene photooxidation have not been reported.

The surface-to-volume (S/V) ratio of the reactor is also an essential factor to vapor wall loss. Lambe et al. (2010) observed that *m*-xylene and α-pinene SOA yields decreased with the increasing flow reactors' S/V ratio (0.23 and 2.8 cm^{-1}). They proposed that the wall losses of SVOCs might partly contribute to the difference of SOA yields. The large smog chambers can allow for a lower concentration and a longer residence time for reactants than the flow reactors. The S/V ratio of a flow reactor is usually larger than that from a chamber; thus, the wall loss rate constants obtained in flow reactors may not be fully applicable to smog chamber studies. Even though the vapor wall losses of OVOCs have been measured in FEP reactors with different S/V ratios from other groups (Finewax et al. 2020; Grosjean, 1985; Krechmer et al., 2016, 2017; Loza et al., 2010; Matsunaga and Ziemann, 2010; McMurry and Grosjean, 1985; Ye et al., 2016; Yeh and Ziemann, 2014, 2015; Zhang et al., 2015), the reactor conditions of these studies vary greatly. To the best of our knowledge, this is the first to compare the effects of different S/V ratios of smog chambers on vapor wall losses of OVOCs from in situ VOC oxidation.

In this study, we studied the wall losses of OVOCs from toluene-H_2O_2-hν systems. The OVOCs were measured by a modified atmospheric pressure chemical ionization mass spectrometer (APCI-MS). The effects of S/V ratios and RH on the wall losses of OVOCs were compared and discussed.

1. Materials and methods

1.1. *Material, monitoring and analysis*

Toluene photooxidation experiments were conducted in a 400 L pillow-shaped and a 5000 L cubic Teflon FEP film reactor in an indoor smog chamber. The light source was supplied by UV lamps (UVA-340, Q-Lab Corporation, USA) to simulate the solar spectrum in the troposphere. The shaded area in the **Fig. S1** represents the overlapping wavelength of UVA-340 lights irradiation and the absorption of H_2O_2. It shows that the H_2O_2 can rapidly decompose to OH radical by UVA-340 light. The effective light intensities in reactors were determined by measuring NO_2 photolysis rate constants, which were 0.16 min^{-1} in 400 L and 0.21 min^{-1} in 5000 L reactors. Our previous works have reported a similar description of the experimental facility (Jia and Xu, 2018, 2020, 2021; Zhang et al., 2019). Here a short description is given.

In all experiments, the background air was generated by a Zero Air Supply (model 111 and model 1150, Thermo Scientific, USA). Two additional hydrocarbon traps (BHT-4, Agilent, USA) were applied in the experiments to purify the air further. The particle mass concentrations were monitored by the scanning electromobility particle sizer (SMPS, Model 3936 TSI, USA), and NO_x concentrations were measured by the NO_x analyzer (Model 42C, Thermo Electron Corporation, USA). NO_x was < 1 ppbV in all experiments, so the effect of NO_x was not considered in this study.

The hydrogen peroxide (H_2O_2, 30 wt.%, Beijing Chemical Works) was used as an OH radical source, and toluene (99.9 wt.% purity, Tanmo Quality Inspection Technology Co., Ltd.) was used as OVOCs precursor. The H_2O_2 and toluene were introduced into the reactor by a microsyringe along with airflow. The zero air (8.5% RH at 296 K) was directly introduced into the FEP reactor for experiments under dry conditions. For experiments under humid conditions (around 70% RH), the RH was controlled by bubbling zero air through high pure water (18.2 MΩ•cm at 298 K, Millipore/Direct-Q3). The RH in the reactor was measured by a hygrometer (Model 645, Testo AG, Lenzkirch, Germany). To ensure that the reactants were well mixed, we kept the reactor in the dark for 25 min (400 L reactor) or 80 min (5000 L reactor) without any activities before

Table 1 – Experimental conditions for toluene-H_2O_2 systems.

Volume of reactor	Experiment No.	S/V (m^{-1})	$[C_7H_8]_0$ (ppmV)	Effective light intensity (min^{-1})	Irradiation time (sec)	Temperature (K)	RH (%)
400 L	1	7.5	2.8	0.16	110	292 ± 1	16.5
	2	7.5	2.8	0.16	90	292 ± 1	66.6
5000 L	3	3.6	2.8	0.21	110	292 ± 1	16.3
	4	3.6	2.8	0.21	90	292 ± 1	69.3

S/V: surface-to-volume (S/V) ratio of the reactor; $[C_7H_8]_0$: initial concentration of C_7H_8 calculated from the amount of toluene and the volume of the reactor; RH: relative humidity in the reactor.

starting each experiment. Then the UV lights were turned on for 110 sec (dry condition) or 90 sec (humid condition) to produce OVOCs from the toluene-H_2O_2 system. No particles were observed before and after the irradiation. We also conducted wall losses experiments with a longer irradiation time (12 - 34 min), and found that particles could be formed after the irradiation. Since the equilibrium time of some OVOCs is less than 30 min, these experiments were not included in this study. To ensure that enough OVOCs could be produced during a short irradiation time, the amounts of H_2O_2 were excessive in all experiments. A modified APCI-MS (Q-Exactive Orbitrap mass spectrometer. Thermo Scientific, Germany) was used to detect the OVOCs in real-time in the negative ion mode. The resolution of APCI-MS was set to 70,000 at a molecular weight (MW) of 200 in the experiments. The flow rate of sample air was 0.3 L/min. All data were acquired and processed using Thermo Scientific Xcalibur software (Thermo Fisher Scientific Inc., USA).

1.2. *Smog chamber experiments*

Two sets of experiments were conducted in a 400 L reactor and a 5000 L reactor to study the wall losses of OVOCs under different S/V ratios and RH conditions (**Table 1**). Though the different shapes of reactors were used, the wall loss rate constants are very close and comparable in the reactors with the same volumes but different shapes from published data (**Table S1**). Therefore, we suppose that the shapes of the reactors may be a minor factor influencing the wall loss. The decays of OVOCs due to wall losses were monitored for 4 - 5 hr at 292 ± 1 K.

The OVOCs in the 400 L reactor were measured online by APCI-MS. In the 400 L reactor, the total sampling volume was 75 L during 4 hr of wall loss experiments. The decrease of reactor volume during sampling may influence the wall loss rates. The results showed that all the objective OVOCs could reach partitioning equilibrium within 1 hr when chamber volume was only reduced by < 20 L. Thus, the change of the reactor volume to the wall loss rates could be neglected. OVOCs in the 5000 L reactor were sampled using a 5 L stainless steel reservoir every 20 min. The sampling flow rate was 7 L/min, and the duration of each sampling was 2.5 min. The sample air in the reservoir was connected to the inlet of APCI-MS within 45 sec. The total sample volume was 300 L. It shows that the chamber volume was almost unchanged during the experimental process in the 5000 L reactor. The sample line was a polytetrafluoroethylene (PTFE) tube (1/4 inch outer diameter, 3/16 inch inner diameter) with a length of 60 cm. The response time was determined to be 0.6 min. The sample tube was so short that the tubing delay effects could be neglected in this study.

Since no particles were observed during the whole experiment, the effect of particle-phase partitioning can be excluded. In addition, since most OH radicals were consumed by toluene when the lights were turned off, thus, most gas-phase oxidation reactions would be excluded. Meanwhile, according to Master Chemical Mechanism (MCM v3.3.1, the website at http://mcm.leeds.ac.uk/MCM; last accessed October 16, 2017) (Saunders et al., 2003), there are no further gas-phase reactions among the OVOCs. Therefore, the decays of OVOCs in the gas phase are mainly due to the wall losses.

2. Results and discussion

When the reactor wall is treated as a phase that organic vapors can partition, then the absorption and the desorption processes of OVOCs between the gas phase and the reactor wall can be represented by first-order reactions (Matsunaga and Ziemann, 2010). This study used a simplified vapor-wall interaction model to study the wall losses of OVOCs formed in toluene-H_2O_2-$h\nu$ systems. The detailed model building and fitting results will be illustrated in the following section.

2.1. *Vapor-wall interaction theory*

The vapor-wall interactions of OVOCs can be expressed as the first-order reversible reactions:

$$OVOC_{i,g} \underset{k_{i,wg}}{\overset{k_{i,gw}}{\rightleftharpoons}} OVOC_{i,w}$$

where $OVOC_{i,g}$ and $OVOC_{i,w}$ are *i*-th OVOC in the gas phase and on the Teflon wall; $k_{i,gw}$ and $k_{i,wg}$ are the corresponding absorption and the desorption rate constants. Based on mass balance, the reaction rate of *i*-th OVOC can be expressed as:

$$\frac{dC_{i,g}}{dt} = -k_{i,gw}C_{i,g} + k_{i,wg}C_{i,w} \quad (1)$$

$$\frac{dC_{i,w}}{dt} = k_{i,gw}C_{i,g} - k_{i,wg}C_{i,w} \quad (2)$$

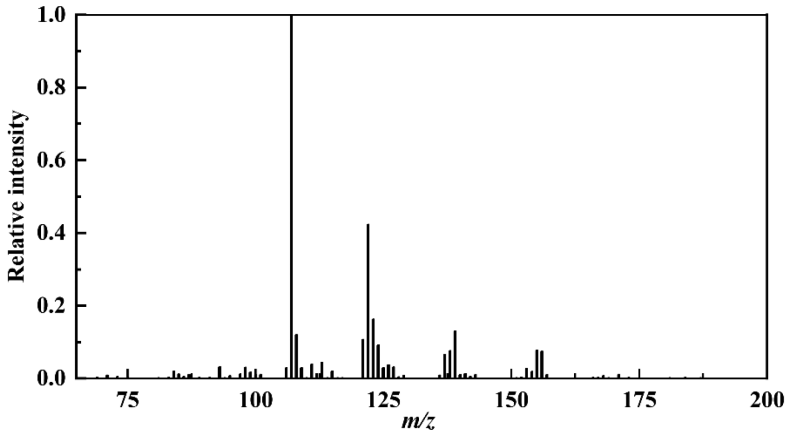

Fig. 1 – Mass spectra of gas-phase OVOCs from toluene photooxidation (in negative mode). *m/z*: mass-to-charge ratio.

where $C_{i,g}$ and $C_{i,w}$ are the concentrations of *i*-th OVOC in the gas phase and on the Teflon wall. The highest concentration of *i*-th OVOC was treated as its initial concentration of wall loss, which is also the total concentration ($C_{i,T}$) of *i*-th OVOC. Because there were no particles in the reactor, $C_{i,T}$ equals to $C_{i,g} + C_{i,w}$ in the process of OVOC wall loss. In our experiments, the gas-phase concentrations of OVOCs were represented by their corresponding ion intensities detected by MS. By solving the Eqs. (1) and (2), $C_{i,g}$ and $C_{i,w}$ can be expressed as a function of time *t*:

$$C_{i,g} = \frac{k_{i,gw}C_{i,T}}{k_{i,gw}+k_{i,wg}} e^{-(k_{i,gw}+k_{i,wg})t} + \frac{k_{i,wg}C_{i,T}}{k_{i,gw}+k_{i,wg}} \quad (3)$$

$$C_{i,w} = -\frac{k_{i,gw}C_{i,T}}{k_{i,gw}+k_{i,wg}} e^{-(k_{i,gw}+k_{i,wg})t} + \frac{k_{i,gw}C_{i,T}}{k_{i,gw}+k_{i,wg}} \quad (4)$$

The values of $k_{i,gw}$ and $k_{i,wg}$ can be obtained by best fitting of the experimental data ($C_{i,g}$, $C_{i,T}$) with Eq. (3). The vapor-wall partitioning equilibrium time ($\tau_{i,gwe}$) for *i*-th OVOC can be calculated by:

$$\tau_{i,gwe} = \frac{1}{k_{i,gw}+k_{i,wg}} \quad (5)$$

Under equilibrium conditions ($\frac{dC_{i,g}}{dt} = 0$), the fraction of *i*-th OVOC lost to the chamber wall ($F_{i,wall}$) can be expressed as:

$$F_{i,wall} = \frac{k_{i,gw}}{k_{i,gw}+k_{i,wg}} \quad (6)$$

2.2. OVOCs from the toluene-H_2O_2 system and their wall loss parameters

The negative mass spectra of gas-phase OVOCs generated by toluene-H_2O_2 irradiation are shown in **Fig. 1**. Total 13 compounds with the signal-to-noise ratios ≥ 3 were analyzed. The molecular weights (MW) of these OVOCs were in a range of 84 to 172 Da. Their molecular structures were proposed based on MCM and published works (**Table 2**). The intensities of these OVOCs gradually decreased with time due to wall losses, and then reached the vapor-wall partitioning equilibrium. These OVOCs are important precursors or monomers of SOA, confirmed by our experimental data and reference reports (Huang et al., 2006; Jang and Kamens, 2001). The average values of k_{gw} and k_{wg} for these OVOCs in 400 and 5000 L reactors are also listed in **Table 3**.

2.3. Vapor wall losses in different S/V reactors

The k_{gw} values of OVOCs in 5000 L reactors are generally smaller than 400 L reactors (**Table 3**). Under dry conditions, the k_{gw} values of all OVOCs are ranged from 0.46×10^{-2} to 2.17×10^{-2} min^{-1}, with an average value of $(0.86 \pm 0.48) \times 10^{-2}$ min^{-1} in the 400 L reactor (S/V = 7.5 m^{-1}); The k_{gw} values are ranged from 0.28×10^{-2} to 0.49×10^{-2} min^{-1}, with an average value of $(0.35 \pm 0.07) \times 10^{-2}$ min^{-1} in 5000 L reactor (S/V = 3.6 m^{-1}). Under humid conditions, the k_{gw} values are ranged from 0.55×10^{-2} to 2.22×10^{-2} min^{-1} (with an average value of $(0.94 \pm 0.47) \times 10^{-2}$ min^{-1}) in 400 L reactor and ranged from 0.31×10^{-2} to 0.58×10^{-2} min^{-1} (with an average value of $(0.39 \pm 0.07) \times 10^{-2}$ min^{-1}) in 5000 L reactor. The average k_{gw} value in the 400 L reactor is about 2.47 (2.41) times larger than that in the 5000 L reactor under the dry (humid) condition. The average k_{wg} value in the 400 L reactor is 1.37 (1.20) times higher than that in the 5000 L reactor under the dry (humid) condition. Therefore, the increase of the S/V ratio can promote the wall losses of OVOCs.

The fraction of OVOC lost to the reactor wall (F_{wall}) can be obtained by Eq. (6) (**Fig. 2**). Under dry (humid) conditions, the F_{wall} values of most OVOCs are in a range of 0.20 - 0.30 (0.30 - 0.40) in the 400 L reactor and 0.10 - 0.20 (0.20 - 0.30) in the 5000 L reactor. The average value of F_{wall} in the 400 L reactor is 1.52 (1.56) times larger than that in the 5000 L reactor under the dry (humid) condition. It shows that the F_{wall} values of MW 84 ($C_4H_4O_2$) and MW 98 ($C_5H_6O_2$) are much higher than other OVOCs in the 400 L reactor. MW 84 and MW 98 are ring-opening carbonyls as shown in **Table 2**. Such conjugated aldehydes are highly reactive (Cao and Jang, 2007), and thus may exhibit more apparent wall losses in the reactor with a larger S/V ratio. By contrast, most ring-retaining OVOCs (e.g. MW 108 (C_7H_8O), 110 ($C_6H_5O_2$), 122 ($C_7H_6O_2$), 124 ($C_7H_8O_2$) 138 ($C_7H_6O_3$)) are less oxidized,

Table 2 – Detected OVOCs from the toluene-H_2O_2-irradiation systems and their potential molecular structures.

No	Molecular weight (MW)	Molecular formula	Proposed molecular structure	References
1	84.020	$C_4H_4O_2$	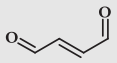	J&K (Jang and Kamens, 2001)
2	94.041	C_6H_6O		MCM
3	98.036	$C_5H_6O_2$	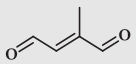	MCM
4	106.041	C_7H_6O	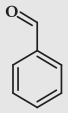	MCM
5	108.057	C_7H_8O	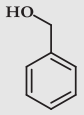	MCM
6	110.036	$C_6H_6O_2$		MCM
7	122.036	$C_7H_6O_2$	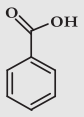	MCM
8	124.052	$C_7H_8O_2$	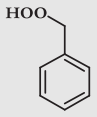	MCM
9	138.031	$C_7H_6O_3$	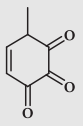	MCM
10	140.047	$C_7H_8O_3$	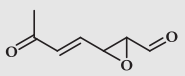	MCM
11	154.026	$C_7H_6O_4$	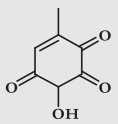	J&K
12	156.042	$C_7H_8O_4$	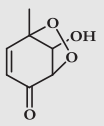	MCM
13	172.037	$C_7H_8O_5$	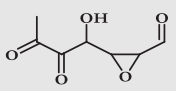	MCM

MCM: Master Chemical Mechanism.

whose wall losses are relatively low and less dependent on S/V ratios.

We further compared the wall loss constants of OVOCs with the reference data. Most products' wall losses were first determined in this study; hence, only a few of them have been studied by others. In some previous studies, the vapor wall losses were treated as the first-order irreversible reactions. We also determined the apparent first-order wall loss rate constants (k_w) of OVOCs based on the irreversible reaction model to compare our data with the reference data. The k_w value of

Table 3 – Values of gas to wall loss rate constant (k_{gw}) and desorption rate constant (k_{wg}) for OVOCs under different S/V ratios and RH conditions.

No.	MW	Molecular formula	Conditions	400 L		5000 L	
				k_{gw} ($\times 10^{-2}$ min^{-1})	k_{wg} ($\times 10^{-2}$ min^{-1})	k_{gw} ($\times 10^{-2}$ min^{-1})	k_{wg} ($\times 10^{-2}$ min^{-1})
1	84	$C_4H_4O_2$	Dry	1.56 ± 0.08	1.83 ± 0.11	0.28 ± 0.05	1.37 ± 0.29
			Humid	1.65 ± 0.06	1.39 ± 0.06	0.34 ± 0.04	1.21 ± 0.19
			Mean	1.61	1.61	0.31	1.29
2	94	C_6H_6O	Dry	1.00 ± 0.06	1.92 ± 0.14	0.41 ± 0.06	1.67 ± 0.29
			Humid	1.06 ± 0.05	1.53 ± 0.08	0.45 ± 0.03	1.09 ± 0.10
			Mean	1.03	1.72	0.43	1.38
3	98	$C_5H_6O_2$	Dry	2.17 ± 0.08	1.75 ± 0.08	0.49 ± 0.05	1.47 ± 0.21
			Humid	2.22 ± 0.08	1.20 ± 0.05	0.58 ± 0.06	1.24 ± 0.17
			Mean	2.19	1.48	0.53	1.35
4	106	C_7H_6O	Dry	0.61 ± 0.04	1.62 ± 0.15	0.28 ± 0.04	1.50 ± 0.26
			Humid	0.65 ± 0.04	1.12 ± 0.08	0.31 ± 0.04	1.26 ± 0.20
			Mean	0.63	1.37	0.30	1.38
5	108	C_7H_8O	Dry	0.55 ± 0.03	2.12 ± 0.14	0.33 ± 0.05	1.66 ± 0.28
			Humid	0.75 ± 0.03	1.59 ± 0.08	0.34 ± 0.05	1.27 ± 0.25
			Mean	0.65	1.85	0.34	1.47
6	110	$C_6H_6O_2$	Dry	1.04 ± 0.15	3.30 ± 0.52	0.39 ± 0.06	1.76 ± 0.33
			Humid	1.13 ± 0.05	2.14 ± 0.12	0.44 ± 0.05	1.41 ± 0.22
			Mean	1.09	2.72	0.41	1.58
7	122	$C_7H_6O_2$	Dry	0.46 ± 0.03	1.93 ± 0.17	0.29 ± 0.04	1.87 ± 0.33
			Humid	0.58 ± 0.02	1.39 ± 0.08	0.34 ± 0.05	1.35 ± 0.29
			Mean	0.52	1.66	0.31	1.61
8	124	$C_7H_8O_2$	Dry	0.50 ± 0.04	1.85 ± 0.16	0.30 ± 0.03	1.61 ± 0.23
			Humid	0.69 ± 0.03	1.59 ± 0.09	0.35 ± 0.04	1.21 ± 0.21
			Mean	0.59	1.72	0.32	1.41
9	138	$C_7H_6O_3$	Dry	0.71 ± 0.07	2.86 ± 0.31	0.28 ± 0.05	1.56 ± 0.33
			Humid	0.80 ± 0.04	1.81 ± 0.12	0.42 ± 0.05	1.32 ± 0.20
			Mean	0.75	2.34	0.35	1.44
10	140	$C_7H_6O_3$	Dry	0.70 ± 0.06	2.57 ± 0.28	0.35 ± 0.04	1.85 ± 0.23
			Humid	0.73 ± 0.03	1.48 ± 0.08	0.37 ± 0.04	1.40 ± 0.18
			Mean	0.71	2.03	0.36	1.63
11	154	$C_7H_6O_4$	Dry	0.80 ± 0.06	2.37 ± 0.19	0.49 ± 0.06	1.61 ± 0.26
			Humid	0.73 ± 0.03	1.23 ± 0.07	0.42 ± 0.04	1.17 ± 0.13
			Mean	0.77	1.8	0.46	1.39
12	156	$C_7H_8O_4$	Dry	0.51 ± 0.04	1.97 ± 0.18	0.33 ± 0.04	1.40 ± 0.22
			Humid	0.55 ± 0.03	1.50 ± 0.10	0.35 ± 0.04	1.30 ± 0.19
			Mean	0.53	1.74	0.34	1.35
13	172	$C_7H_8O_5$	Dry	0.58 ± 0.05	1.82 ± 0.20	0.30 ± 0.05	1.12 ± 0.26
			Humid	0.65 ± 0.03	1.34 ± 0.08	0.36 ± 0.04	0.91 ± 0.15
			Mean	0.61	1.58	0.33	1.01

MW 122 (108) is determined to be 1.2×10^{-5} sec^{-1} (1.5×10^{-5} sec^{-1}) in 5000 L reactor, which is very close to the reference value of 1.8×10^{-5} sec^{-1} ($< 0.6 \times 10^{-5}$ sec^{-1}) in a 3900 L reactor (S/V = 3.8 m^{-1}, under dry condition) (Grosjean, 1985). In addition, the correlation between experimental data and the fitted line by the reversible reaction model is much better than that based on the irreversible reaction model (**Fig. 3**); thus, it is more reasonable to treat the vapor wall loss processes as the reversible reactions.

By in-situ photooxidation of toluene-H_2O_2, Zhang et al. (2015) measured the wall loss rate constants of MW 122 ($C_7H_6O_2$) and 124 ($C_7H_8O_2$) based on first-order irreversible reaction model in a dual 24 m^3 reactors under dry conditions. The k_w values of MW 122 and 124 were $(2.0 \pm 1.9) \times 10^{-6}$ and $(5.8 \pm 1.9) \times 10^{-6}$ sec^{-1}, respectively. In our study, the corresponding k_w values of MW 122 and 124 were $(1.2 \pm 0.12) \times 10^{-5}$ and $(1.4 \pm 0.13) \times 10^{-5}$ sec^{-1} in 5000 L reactor at 16.3% RH. It shows that the k_w value of MW 122 (124) is 6.0 (2.4) times larger than that in Zhang et al.'s work (Zhang et al., 2015). This may be due to the relatively small reactor volume in our work; Besides, different lengths of initial irradiation time may lead to varying definitions of the initial points of wall decays (Krechmer et al. 2016).

2.4. *Vapor wall losses under different RH conditions*

The values of k_{gw} under humid conditions are slightly higher than that under dry conditions for most OVOCs. The average k_{gw} value under the humid condition is 1.09 (1.12) times higher than that under the dry condition in the 400 L (5000 L) reactor. It shows that the effect of RH on k_{gw} is not apparent in both 400 and 5000 L reactors. The forward reaction rate of k_{gw} is mainly dependent on the gas-phase diffusion rate of molecules, which is a function of molecular

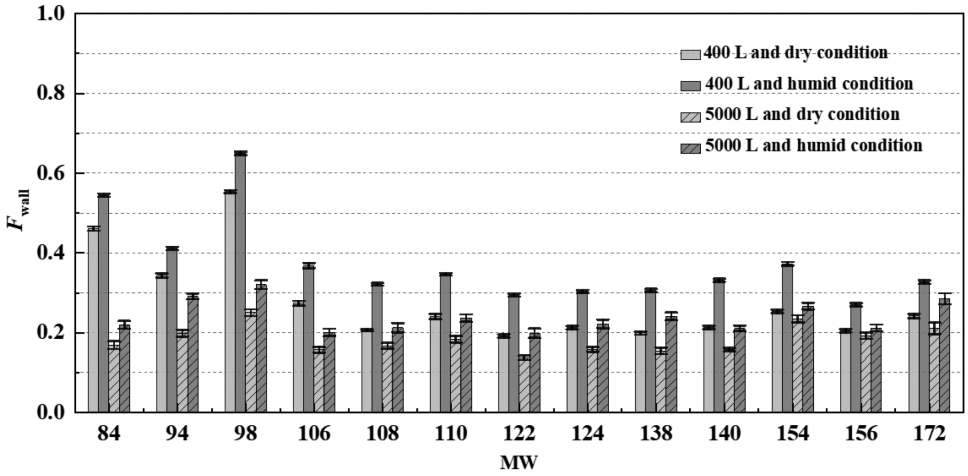

Fig. 2 – The fraction of OVOC lost to the reactor wall (F_{wall}) in 400 and 5000 L reactors under both dry (16.5% RH) and humid (70.0% RH) conditions.

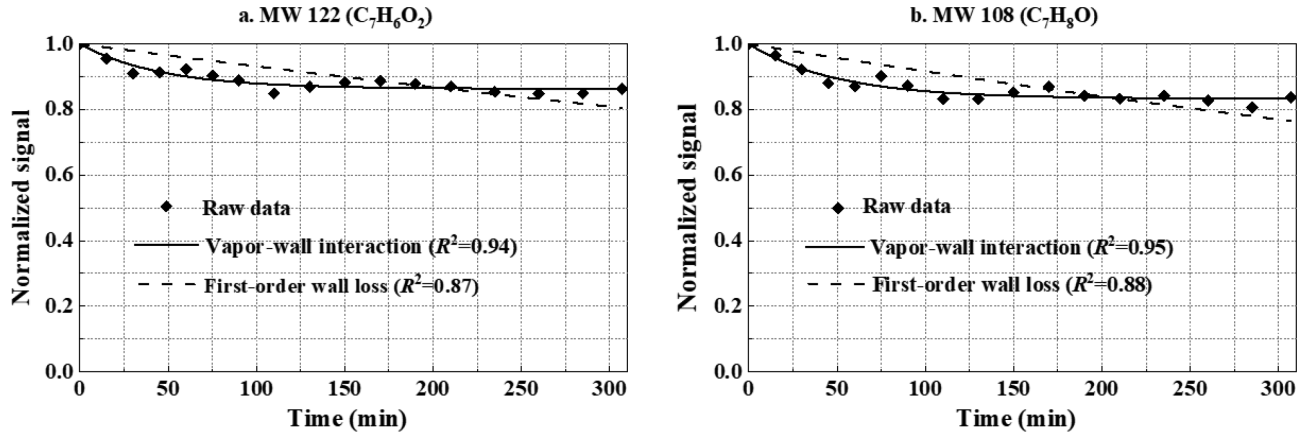

Fig. 3 – Wall losses of MW (a) 122 and (b) 108 in 5000 L reactor at 16.3% RH based on the reversible (solid line) and irreversible reaction model (dash line).

weight (MW); thus, the effect of RH on k_{gw} is not remarkable. However, the average k_{wg} value under the dry condition is 1.45 (1.27) times higher than that under the humid condition in the 400 L (5000 L) reactor. The molecular structures of these OVOCs can well explain it. Since OVOCs were produced by oxidation of toluene, these OVOCs always contain polar functional groups and should be water-soluble. Hence, the interactions of OVOCs with humid reactor surfaces decreased the desorption rates of OVOCs. In addition, the average F_{wall} value under the humid condition is 1.35 (1.32) times higher than that under the dry condition in the 400 L (5000 L) reactor. For comparison, we also determined the k_w values of all OVOCs in our study. The average k_w values of all OVOCs in 5000 L reactor are (1.6 ± 0.3) × 10^{-5} sec^{-1} (dry) and (2.2 ± 0.3) × 10^{-5} sec^{-1} (humid), respectively. Loza et al. (2010) measured the RH-dependent wall loss of 2,3-epoxy-1,4-butanediol ($C_4H_8O_3$) in dual 28 m^3 reactors and obtained the values of 3.7 × 10^{-5} sec^{-1} at 10% RH and around 7.4 × 10^{-5} sec^{-1} at 45% RH. The effect of RH on k_w value in this study is close to Loza et al. (2010).

2.5. *Effects of S/V and RH on τ_{gwe} values*

The τ_{gwe} value can reflect both the forward and the reverse reaction rates of the OVOC wall loss process. Under dry conditions, the τ_{gwe} values are ranged from 23.0 to 45.0 min, with an average value of (34.7 ± 7.0) min in 400 L reactor, and in a range of 45.5 to 70.8 min in 5000 L reactor (with an average value of (52.9 ± 6.9) min); Under humid conditions, the τ_{gwe} values are ranged from 29.3 to 56.7 min (with an average value of (43.0 ± 8.3) min) in 400 L reactor and in a range of 54.2 to 79.0 min (with an average value of (61.9 ± 6.1) min) in 5000 L reactor. The average τ_{gwe} value is 1.52 (1.44) times higher in 5000 L reactor than that in 400 L reactor under the dry (humid) condition. The average τ_{gwe} value is 1.24 (1.17) times higher under humid conditions than under dry conditions in the 400 L (5000 L) reactor. Overall, it takes much longer for most OVOCs to reach partitioning equilibrium in the reactor with a smaller S/V ratio and under humid conditions (**Fig. 4**).

Ziemann and co-workers (Matsunaga and Ziemann, 2010; Yeh and Ziemann, 2014, 2015) measured the τ_{gwe} values of 1-

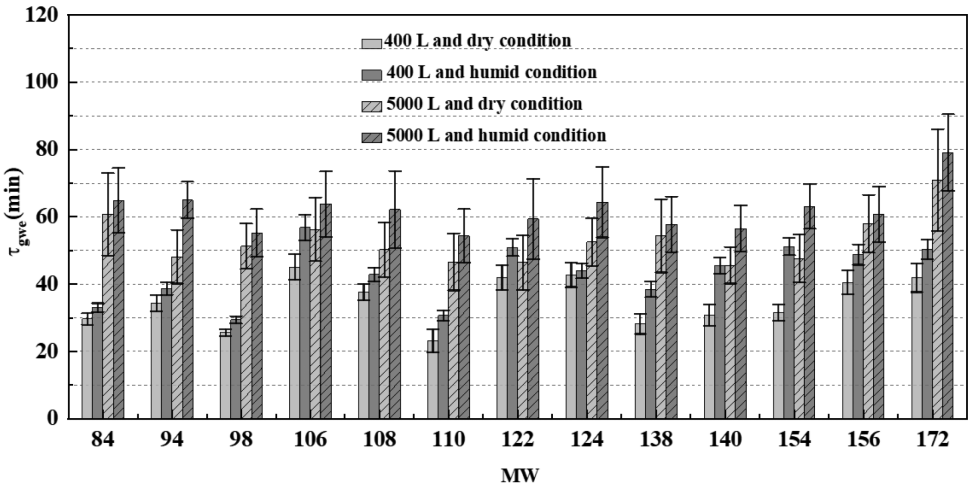

Fig. 4 – Vapor-wall partitioning equilibrium time (τ_{gwe}) values of OVOCs in 400 and 5000 L reactors under dry (16.5% RH) and humid (70.0% RH) conditions.

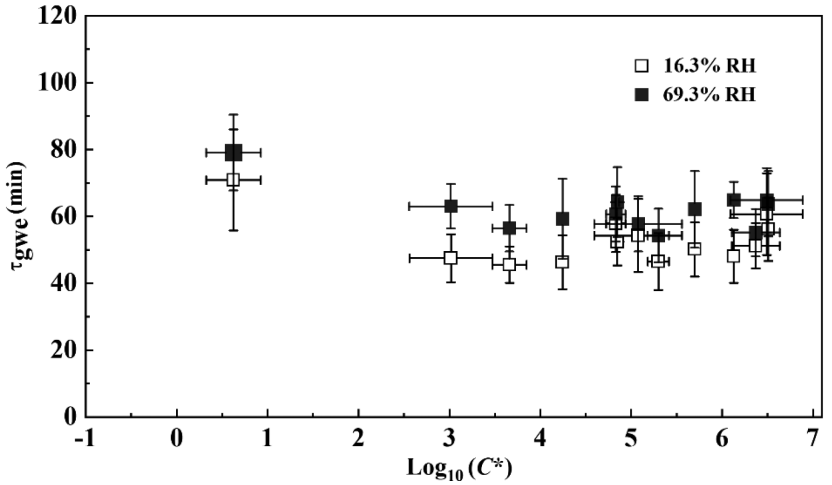

Fig. 5 – Relationship between vapor-wall partitioning equilibrium time (τ_{gwe}) and saturation concentration (in the form of $\log_{10}(C^*)$) of OVOCs. The error bars in the *x*-axis direction denote the standard error of the mean.

alkenes, ketones, alcohols, monoacids, diols (with MW range of 90 - 226) and alkyl nitrates (with MW range of 175 - 259) in an 8.2 m^3 reactor at 296 - 300 K and at < 1% RH, in which the τ_{gwe} values are in a range of 8 to 140 min. It shows that all the τ_{gwe} values in our study (23 - 79 min) fall within the range of Ziemann and co-workers. **Fig. 5** shows the experimentally determined and estimated saturation concentration (in the form of $\log_{10}(C^*)$) of OVOCs based on a functional group contribution method. The vapor pressures of phenol (MW 94), *o*-cresol (MW 108), benzaldehyde (MW 106) and benzoic acid (MW 122) are referred to the summary of Asher and Pankow (2006). The vapor pressures of other OVOCs at 292 K listed in **Table 2** are calculated by an online model UmanSysProp v1.0 (Topping et al., 2016). In this model, the vapor pressure method is described by Nannoolal (2008), and boiling point methods are described by Nannoola and Stein and Brown (Nannoolal et al., 2004; Stein and Brown, 1994). The C^* values of OVOCs in this study are determined to be mainly 10^2 - 10^7 $\mu g/m^3$, which is similar to the range of 10^3 - 10^7 $\mu g/m^3$ in Ziemann and co-workers' work. Krechmer et al. (2016) generated hydroxynitrates (with MW range of 193 - 247) from the oxidation of 1-alcohols (n_C = 6 - 12) in an 8 m^3 reactor at 295 K under dry conditions. The C^* values of these hydroxynitrates are 10^{-1} - 10^3 $\mu g/m^3$. Their τ_{gwe} values were 7 - 13 min, which is smaller than ours. The types of oxidized organic compounds may lead to the difference. Besides, the temperature in the study of krechmer et al. was controlled 2 - 3 K higher than ours, which might accelerate the partitioning process.

Zhang et al. (2015) measured the time scales for wall deposition (τ_w) of 25 OVOCs from the oxidation of isoprene, toluene, α-pinene, and dodecane in dual 24 m^3 reactors under dry conditions. The rate constants were obtained based on the first-order irreversible reaction model, in which the τ_w values were ranged from around 10 min to 6 days. We also determined the τ_w values based on the irreversible reaction model and found that the τ_w values ranged from around 12 hr (average) to 24 hr in the 5000 L reactor at 16.3% RH. It shows that the va-

por wall loss model can significantly influence the time scales for wall deposition. In addition, the initial irradiation time is much longer in Zhang et al.'s work (about 1 - 7 hr) than that in our study (90 and 110 sec), which may also be a reason for the larger τ_w value from Zhang et al.'s study than ours (Krechmer et al., 2016).

3. Conclusions

Toluene is the simplest and most abundant alkyl aromatics in the atmosphere of China. Various OVOCs can be formed from toluene photooxidation. Then these OVOCs can partition into particle phase and account for a significant portion of SOA. However, these OVOCs can also partition to the reactor walls, affecting the final SOA yields in the chamber experiments and further biasing the estimation of SOA yields. This study studied the vapor-wall interactions of OVOCs generated from toluene-H_2O_2-$h\nu$ systems on short time scales in different S/V ratios of reactors and different RH conditions. The results show that the increase of the S/V ratio can promote the wall losses of OVOCs. The average k_{gw} value in a 400 L reactor is 2.47 (2.41) times higher than in a 5000 L reactor under dry (humid) conditions. Correspondingly, the average k_{wg} value of OVOCs in the 400 L reactor is 1.37 (1.20) times higher than that in the 5000 L reactor under dry (humid) conditions. The increase of RH exerts a weak influence on k_{gw} values. The average k_{gw} value is only 1.09 (1.12) times higher under humid conditions than under dry conditions in the 400 L (5000 L) reactors. However, increasing RH can decrease the desorption rate constant k_{wg}. The average k_{wg} value under dry conditions is 1.45 (1.27) times higher than under humid conditions in the 400 L (5000 L) reactors. Increasing RH can increase the timescales to reach partitioning equilibrium. The average τ_{gwe} value is 1.24 (1.17) times higher under humid conditions than under dry conditions in the 400 L (5000 L) reactor, thereby enhancing the wall losses of OVOCs under humid conditions at equilibrium. Under dry (humid) conditions, the fractions of OVOCs lost to the reactor wall are in a range of 0.20 - 0.30 (0.30 - 0.40) in the 400 L reactor and 0.10 - 0.20 (0.20 - 0.30) in 5000 L reactor.

Acknowledgments

This work was supported by the National Key R&D Program of China (No. 2017YFC0210005) and the National Natural Science Foundation of China (Nos. 41875166, 41875163 and 41375129).

Appendix A Supplementary data

Supplementary material associated with this article can be found in the online version at doi:10.1016/j.jes.2021.09.026.

REFERENCES

Asher, W.E., Pankow, J.F., 2006. Vapor pressure prediction for alkenoic and aromatic organic compounds by a UNIFAC-based group contribution method. Atmos. Environ. 40, 3588–3600.

Bates, K.H., Crounse, J.D., St. Clair, J.M., Bennett, N.B., Nguyen, T.B., Seinfeld, J.H., et al., 2014. Gas phase production and loss of isoprene epoxydiols. J. Phys. Chem. A 118 (7), 1237–1246.

Bertrand, A., Temime-Roussel, B., Wortham, H., Marchand, N., Stefenelli, G., Pieber, S.M., et al., 2018. Influence of the vapor wall loss on the degradation rate constants in chamber experiments of levoglucosan and other biomass burning markers. Atmos. Chem. Phys. 18 (15), 10915–10930.

Cao, G., Jang, M., 2007. Effects of particle acidity and UV light on secondary organic aerosol formation from oxidation of aromatics in the absence of NOx. Atmos. Environ. 41 (35), 7603–7613.

Chen, T.Z., Liu, Y.C., Chu, B.W., Liu, C.G., Liu, J., Ge, Y.L., et al., 2019. Differences of the oxidation process and secondary organic aerosol formation at low and high precursor concentrations. J. Environ. Sci. 79, 256–263.

Chen, T.Z., Chu, B.W., Ma, Q.X., Zhang, P., Liu, J., He, H., 2021. Effect of relative humidity on SOA formation from aromatic hydrocarbons: Implications from the evolution of gas- and particle-phase species. Sci. Total Environ. 773, 145015.

Finewax, Z., Jimenez, J.L., Ziemann, P.J., 2020. Development and application of a low-cost vaporizer for rapid, quantitative, in situ addition of organic gases and particles to an environmental chamber. Aerosol Sci. Technol. 54 (12), 1567–1578.

Grieshop, A.P., Miracolo, M.A., Donahue, N.M., Robinson, A.L., 2009. Constraining the volatility distribution and gas-particle partitioning of combustion aerosols using isothermal dilution and thermodenuder measurements. Environ. Sci. Technol. 43 (13), 4750–4756.

Grosjean, D., 1985. Wall loss of gaseous pollutants in outdoor Teflon chambers. Environ. Sci. Technol. 19 (11), 1059–1065.

Huang, M.Q., Zhang, W.J., Hao, L.Q., Wang, Z.Y., Zhou, L.Z., Gu, X.J., et al., 2006. Chemical composition and reaction mechanisms for secondary organic aerosol from photooxidation of toluene. J. Chin. Chem. Soc. 53 (5), 1149–1156.

Huang, M.Q., Zhang, J.H., Cai, S.Y., Liao, Y.M., Zhao, W.X., Hu, C.J., et al., 2016. Characterization of particulate products for aging of ethylbenzene secondary organic aerosol in the presence of ammonium sulfate seed aerosol. J. Environ. Sci. 47, 219–229.

Huang, Y.L., Zhao, R., Charan, S.M., Kenseth, C.M., Zhang, X., Seinfeld, J.H., 2018. Unified theory of vapor-wall Mass transport in Teflon-walled environmental chambers. Environ. Sci. Technol. 52 (4), 2134–2142.

Huffman, J.A., Docherty, K.S., Aiken, A.C., Cubison, M.J., Ulbrich, I.M., Decarlo, P.F., et al., 2009. Chemically-resolved aerosol volatility measurements from two megacity field studies. Atmos. Chem. Phys. 9 (18), 7161–7182.

Jang, M., Kamens, R.M., 2001. Characterization of secondary aerosol from the photooxidation of toluene in the presence of NOx and 1-propene. Environ. Sci. Technol. 35 (18), 3626–3639.

Jia, L., Xu, Y.F., 2018. Different roles of water in secondary organic aerosol formation from toluene and isoprene. Atmos. Chem. Phys. 18 (11), 8137–8154.

Jia, L., Xu, Y.F., 2020. The role of functional groups in the understanding of secondary organic aerosol formation mechanism from α-pinene. Sci. Total Environ. 738, 139831.

Jia, L., Xu, Y.F., 2021. A Core-Shell box model for simulating Viscosity dependent secondary organic Aerosol (CSVA) and its application. Sci. Total Environ. 789, 147954.

Kokkola, H., Yli-Pirila, P., Vesterinen, M., Korhonen, H., Keskinen, H., Romakkaniemi, S., et al., 2014. The role of low volatile organics on secondary organic aerosol formation. Atmos. Chem. Phys. 14 (3), 1689–1700.

Krechmer, J.E., Pagonis, D., Ziemann, P.J., Jimenez, J.L., 2016. Quantification of gas-wall partitioning in Teflon environmental Chambers using rapid bursts of low-volatility oxidized species generated in situ. Environ. Sci. Technol. 50 (11), 5757–5765.

Krechmer, J.E., Day, D.A., Ziemann, P.J., Jimenez, J.L., 2017. Direct measurements of gas/particle partitioning and mass accommodation coefficients in environmental chambers. Environ. Sci. Technol. 51 (20), 11867–11875.

Kroll, J.H., Chan, A.W.H., Ng, N.L., Flagan, R.C., Seinfeld, J.H., 2007. Reactions of semivolatile organics and their effects on secondary organic aerosol formation. Environ. Sci. Technol. 41 (10), 3545–3550.

La, Y.S., Camredon, M., Ziemann, P.J., Valorso, R., Matsunaga, A., Lannuque, V., et al., 2016. Impact of chamber wall loss of gaseous organic compounds on secondary organic aerosol formation : explicit modeling of SOA formation from alkane and alkene oxidation. Atmos. Chem. Phys. 16 (3), 1417–1431.

Lambe, A.T., Ahern, A.T., Williams, L.R., Slowik, J.G., Wong, J.P.S., Abbatt, J.P.D., et al., 2010. Characterization of aerosol photooxidation flow reactors: heterogeneous oxidation, secondary organic aerosol formation and cloud condensation nuclei activity measurements. Atmos. Meas. Tech. 4 (3), 445–461.

Liao, H., Henze, D.K., Seinfeld, J.H., Wu, S., Mickley, L.J., 2007. Biogenic secondary organic aerosol over the United States: Comparison of climatological simulations with observations. J. Geophys. Res. Atmos. 112, 1–19.

Liu, S.J., Tsona, N.T., Zhang, Q., Jia, L., Xu, Y.F., Du, L., 2019. Influence of relative humidity on cyclohexene SOA formation from OH photooxidation. Chemosphere 231, 478–486.

Loza, C.L., Chan, A.W.H., Galloway, M.M., Keutsch, F.N., Flagan, R.C., Seinfeld, J.H., 2010. Characterization of vapor wall loss in laboratory chambers. Environ. Sci. Technol. 44 (13), 5074–5078.

Matsunaga, A., Ziemann, P.J., 2010. Gas-wall partitioning of organic compounds in a teflon film chamber and potential effects on reaction product and aerosol yield measurements. Aerosol Sci. Technol. 44 (10), 881–892.

McMurry, P.H., Grosjean, D., 1985. Gas and aerosol wall losses in Teflon film smog chambers. Environ. Sci. Technol. 19 (12), 1176–1182.

McVay, R.C., Cappa, C.D., Seinfeld, J.H., 2014. Vapor-wall deposition in chambers: Theoretical considerations. Environ. Sci. Technol. 48 (17), 10251–10258.

Nah, T., McVay, R.C., Zhang, X., Boyd, C.M., Seinfeld, J.H., Ng, N.L., 2016. Influence of seed aerosol surface area and oxidation rate on vapor wall deposition and SOA mass yields: A case study with α-pinene ozonolysis. Atmos. Chem. Phys. 16 (14), 9361–9379.

Nannoolal, Y., Rarey, J., Ramjugernath, D., Cordes, W., 2004. Estimation of pure component properties: Part 1. Estimation of the normal boiling point of non-electrolyte organic compounds via group contributions and group interactions. Fluid Phase Equilib. 226, 45–63.

Nannoolal, Y., Rarey, J., Ramjugernath, D., 2008. Estimation of pure component properties part 3. Estimation of the vapor pressure of non-electrolyte organic compounds via group contribution and group interactions. Fluid Phase Equilib. 269 (1–2), 117–133.

Nguyen, T.B., Coggon, M.M., Bates, K.H., Zhang, X., Schwantes, R.H., Schilling, K.A., et al., 2014. Organic aerosol formation from the reactive uptake of isoprene epoxydiols (IEPOX) onto non-acidified inorganic seeds. Atmos. Chem. Phys. 14 (7), 3497–3510.

Nguyen, T.B., Tyndall, G.S., Crounse, J.D., Teng, A.P., Bates, K.H., Schwantes, R.H., et al., 2016. Atmospheric fates of Criegee intermediates in the ozonolysis of isoprene. Phys. Chem. Chem. Phys. 18 (15), 10241–10254.

Pan, X.L., Uno, I., Wang, Z, Nishizawa, T., Sugimoto, N., Yamamoto, S., et al., 2017. Real-time observational evidence of changing Asian dust morphology with the mixing of heavy anthropogenic pollution. Sci. Rep. 7, 335.

Pathak, R., Donahue, N.M., Pandis, S.N., 2008. Ozonolysis of β-pinene: Temperature dependence of secondary organic aerosol mass fraction. Environ. Sci. Technol. 42 (14), 5081–5086.

Saunders, S.M., Jenkin, M.E., Derwent, R.G., Pilling, M.J., 2003. Protocol for the development of the master chemical mechanism, MCM v3 (Part A): tropospheric degradation of non-aromatic volatile organic compounds. Atmos. Chem. Phys. 3, 161–180.

Shi, B., Wang, W.G., Zhou, L., Li, J.L., Wang, J., Chen, Y., et al., 2019. Kinetics and mechanisms of the gas-phase reactions of OH radicals with three C_{15} alkanes. Atmos. Environ. 207, 75–81.

Song, M., Zhang, C.L., Wu, H., Mu, Y.J., Ma, Z.B., Zhang, Y.Y., et al., 2019. The influence of OH concentration on SOA formation from isoprene photooxidation. Sci. Total Environ. 650, 951–957.

Stein, S.E., Brown, R.L., 1994. Estimation of normal boiling points from group contributions. J. Chem. Inf. Comput Sci. 34 (3), 581–587.

Steinfeld, J.I., 1998. Atmospheric chemistry and physics: From air pollution to climate change. Environ. Sci. Policy Sustain. Dev. 40, 26.

Suda, S.R., Petters, M.D., Yeh, G.K., Strollo, C., Matsunaga, A., Faulhaber, A., et al., 2014. Influence of functional groups on organic aerosol cloud condensation nucleus activity. Environ. Sci. Technol. 48 (17), 10182–10190.

Topping, D., Barley, M., Bane, M.K., Higham, N., Aumont, B., Dingle, N., et al., 2016. UManSysProp v1.0: an online and open-source facility for molecular property prediction and atmospheric aerosol calculations. Geosci. Geosci. Model Dev. 9, 899–914.

Wang, W.G., Li, K., Zhou, L., Ge, M.F., Hou, S.Q., Tong, S.R., et al., 2015. Evaluation and application of dual-reactor chamber for studying atmospheric oxidation processes and mechanisms. Acta Phys. Chim. Sin. 31 (7), 1251–1259.

Wang, X.M., Liu, T.Y., Bernard, F., Ding, X., Wen, S.X., Zhang, Y.L., et al., 2014. Design and characterization of a smog chamber for studying gas-phase chemical mechanisms and aerosol formation. Atmos. Meas. Tech. 7 (1), 301–313.

Ye, P., Ding, X., Hakala, J., Hofbauer, V., Robinson, E.S., Donahue, N.M., 2016. Vapor wall loss of semivolatile organic compounds in a Teflon chamber. Aerosol Sci. Technol. 50 (8), 822–834.

Yeh, G.K., Ziemann, P.J., 2014. Alkyl nitrate formation from the reactions of C_8-C_{14} n-Alkanes with OH radicals in the presence of NOx: Measured yields with essential corrections for gas-wall partitioning. J. Phys. Chem. A 118 (37), 8147–8157.

Yeh, G.K., Ziemann, P.J., 2015. Gas-wall partitioning of oxygenated organic compounds: Measurements, structure-activity relationships, and correlation with gas chromatographic retention factor. Aerosol Sci. Technol. 49 (9), 727–738.

Zhang, Q., Xu, Y.F., Jia, L., 2019. Secondary organic aerosol formation from OH-initiated oxidation of m-xylene: effects of relative humidity on yield and chemical composition. Atmos. Chem. Phys. 19 (23), 15007–15021.

Zhang, X., Cappa, C.D., Jathar, S.H., McVay, R.C., Ensberg, J.J., Kleeman, M.J., et al., 2014. Influence of vapor wall loss in laboratory chambers on yields of secondary organic aerosol. Proc. Natl. Acad. Sci. 111 (16), 5802–5807.

Zhang, X., Schwantes, R.H., McVay, R.C., Lignell, H., Coggon, M.M., Flagan, R.C., et al., 2015. Vapor wall deposition in Teflon chambers. Atmos. Chem. Phys. 15 (8), 4197–4214.